



## Sound velocities of ferropericlase in the Earth's lower mantle

Jung-Fu Lin,<sup>1</sup> Steven D. Jacobsen,<sup>2,3</sup> Wolfgang Sturhahn,<sup>4</sup> Jennifer M. Jackson,<sup>2,5</sup> Jiyong Zhao,<sup>4</sup> and Choong-Shik Yoo<sup>1</sup>

Received 6 September 2006; revised 6 October 2006; accepted 18 October 2006; published 18 November 2006.

[1] Sound velocity measurements on candidate mantle minerals at relevant mantle conditions are needed to interpret Earth's seismic structure in terms of model abundances, variable composition, and other potentially influential parameters such as electronic spin-pairing transitions. Here the sound velocities of the lower-mantle ferropericlase have been measured by nuclear resonant inelastic X-ray scattering to 110 GPa. Compressional and shear wave velocities and their pressure derivatives rise dramatically across the spin-pairing transition of iron in (Mg<sub>0.75</sub>Fe<sub>0.25</sub>)O above 50 GPa. Effects of the transition on the sound velocities of (Mg, Fe)O at lower-mantle pressures yield values that are much greater than what is predicted by studying pure MgO and high-spin ferropericlase. Our results indicate that sound velocities of the low-spin ferropericlase need to be considered in future geophysical and geochemical models, which could offset the effect of the addition of iron in the lower-mantle minerals and affect the evaluation of the lower-mantle heterogeneities.

**Citation:** Lin, J.-F., S. D. Jacobsen, W. Sturhahn, J. M. Jackson, J. Zhao, and C.-S. Yoo (2006), Sound velocities of ferropericlase in the Earth's lower mantle, *Geophys. Res. Lett.*, 33, L22304, doi:10.1029/2006GL028099.

### 1. Introduction

[2] The speed of seismic waves in the Earth's lower mantle is governed by the elastic properties of an assemblage thought to consist mainly of ~20% ferropericlase and ~80% silicate perovskite [e.g., *Dziewonski and Anderson*, 1981; *Jackson*, 1998; *Kellogg et al.*, 1999; *van der Hilst and Kárason*, 1999; *Trampert et al.*, 2004; *Wentcovitch et al.*, 2004; *Li and Zhang*, 2005]. Knowledge of the sound velocities of ferropericlase and silicate perovskite at high pressures and temperatures is thus essential to the understanding of the geophysics and geochemistry of the Earth's lower mantle. However, experimental studies on the sound velocities of ferropericlase-(Mg, Fe)O have been restricted to pressures below about 20 GPa [*Zha et al.*, 2000; *Jacobsen et al.*, 2002, 2004; *Kung et al.*, 2002; *Jackson et al.*, 2006] and therefore may not reflect the properties of

lower-mantle (Mg, Fe)O with iron in the pressure-induced low-spin state [e.g., *Badro et al.*, 2003, 2004; *Li et al.*, 2004; *Fei et al.*, 2005; *Jackson et al.*, 2005; *Lin et al.*, 2005, 2006; *Sturhahn et al.*, 2005; *Speziale et al.*, 2005; *Goncharov et al.*, 2006; *Hofmeister*, 2006; *Tsuchiya et al.*, 2006]. Since ferropericlase is considered to constitute a considerable volume fraction of the lower mantle (~20%) and is probably iron-rich compared with silicate perovskite [*Murakami et al.*, 2005], an understanding of the effects of the electronic spin-pairing transition on the sound velocities and transport properties of (Mg, Fe)O is crucial to modeling deep-Earth geodynamics and geochemistry [*Mattern et al.*, 2005; *Goncharov et al.*, 2006].

[3] A recent X-ray diffraction study of (Mg<sub>0.83</sub>, Fe<sub>0.17</sub>)O to 135 GPa showed a dramatic increase in the isothermal bulk modulus ( $K_T$ ) and bulk sound velocity ( $V_\Phi$ ) at the electronic spin-pairing transition [*Lin et al.*, 2005], but compressional ( $V_P$ ) and shear ( $V_S$ ) wave velocities and shear modulus ( $G$ ) of the low-spin ferropericlase have not previously been measured. Here we have measured the partial phonon densities of states (PDOS) of iron in (Mg<sub>0.75</sub>, Fe<sub>0.25</sub>)O by nuclear resonant inelastic X-ray scattering (NRIXS) [*Sturhahn*, 2004] to pressures exceeding one megabar. We have derived the  $V_P$ ,  $V_S$ , and  $G$  of the high-spin and low-spin ferropericlase from the PDOS. NRIXS, using a high-intensity synchrotron X-ray source, probes the PDOS for <sup>57</sup>Fe incorporated into <sup>57</sup>Fe-bearing samples [*Sturhahn*, 2004], and has been used with a diamond-anvil cell to determine the elastic, thermodynamic, and vibrational properties of <sup>57</sup>Fe-containing materials at high pressure [*Hu et al.*, 2003; *Mao et al.*, 2004].

### 2. Experiments

[4] High-pressure NRIXS experiments were conducted at sector 3 of the Advanced Photon Source (APS), Argonne National Laboratory (ANL). Energy spectra were obtained by tuning the X-ray energy ( $\pm 70$  meV to  $\pm 90$  meV in steps of 0.25 meV) around the nuclear transition energy of 14.4125 keV with an energy resolution of 1 meV. The Fe- $K_{\alpha,\beta}$  fluorescence radiation from the <sup>57</sup>Fe-enriched (Mg<sub>0.75</sub>, Fe<sub>0.25</sub>)O polycrystalline sample, emitted with time delay relative to the incident X-ray pulses due to the lattice excitations of the iron sublattice, was collected by three avalanche photodiode detectors.

[5] Polycrystalline (Mg<sub>0.75</sub>, Fe<sub>0.25</sub>)O with ~95% enrichment in <sup>57</sup>Fe was synthesized in an oxygen fugacity controlled gas-mixing furnace [*Jacobsen et al.*, 2002; *Lin et al.*, 2006]. For experiments below 33 GPa, the sample was loaded into the sample chamber of a diamond anvil cell (DAC) with a neon pressure medium and a few ruby spheres. For experiments above 33 GPa, a perforated diamond having 100  $\mu\text{m}$  inner culet, 300  $\mu\text{m}$  outer culet,

<sup>1</sup>Lawrence Livermore National Laboratory, Livermore, California, USA.

<sup>2</sup>Geophysical Laboratory, Carnegie Institution of Washington, Washington, D. C., USA.

<sup>3</sup>Department of Earth and Planetary Sciences, Northwestern University, Evanston, Illinois, USA.

<sup>4</sup>Advanced Photon Source, Argonne National Laboratory, Argonne, Illinois, USA.

<sup>5</sup>Now at Division of Geological and Planetary Sciences, California Institute of Technology, Pasadena, California, USA.

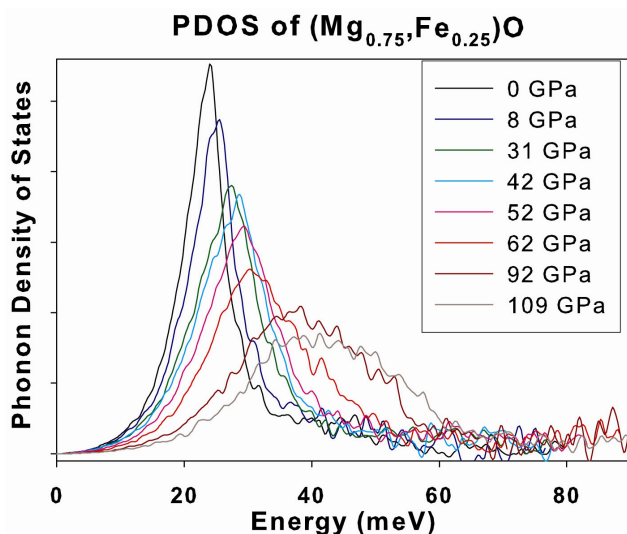


**Figure 1.** PDOS of  $(\text{Mg}_{0.75}, \text{Fe}_{0.25})\text{O}$  under high pressures. The spectral features of PDOS are shifted to higher energies with increasing pressure, whereas the energy shift is much more significant across the electronic spin-pairing transition from 42 to 62 GPa. The low-energy slope of the PDOS in the range of 0.2 meV to 15 meV is used to derive the bulk Debye sound velocity ( $V_D$ ) [Hu *et al.*, 2003].

and a bevel angle of 9 degrees on the side of the incident X-ray beam was used to reduce absorption by the anvil, allowing NRIXS spectra to be collected within a reasonable time frame of less than a day. A beryllium gasket of 3 mm in diameter was pre-indented to a thickness of 30  $\mu\text{m}$  and a hole of 250  $\mu\text{m}$  was drilled in it. Subsequently, amorphous boron powder was inserted into the drilled hole and a smaller hole of 50  $\mu\text{m}$  in diameter was drilled and used as the sample chamber [Lin *et al.*, 2003]. Use of the boron gasket insert helps to strengthen the Be gasket, increase the sample volume, and reduce the axial pressure gradients. The very small and highly focused X-ray beam of less than 10  $\mu\text{m}$  in diameter also helps to reduce the pressure uncertainty caused by the radial pressure gradient. Pressures were determined using the ruby fluorescence scale, and the pressure uncertainty ( $1\sigma$ ) was estimated from multiple pressure measurements from the ruby balls in the sample chamber. The counting time for each NRIXS spectrum was approximately one hour, and ten to twenty spectra were collected and added at each pressure.

### 3. Results and Discussion

[6] A quasi-harmonic model was used to extract the PDOS from the measured energy spectra (Figure 1) [Sturhahn, 2004]. While the integration of the PDOS gives the elastic, thermodynamic, and vibrational parameters from the contribution of the iron atoms in  $(\text{Mg}_{0.75}, \text{Fe}_{0.25})\text{O}$ , the bulk Debye sound velocity ( $V_D$ ) of the sample is derived from parabolic fitting of the low-energy slope of the PDOS in the range of approximately 0.2 meV to 15 meV after applying a correction factor, the cube root of the ratio of the mass of the nuclear resonant isotope ( $^{57}\text{Fe}$ ) to the average atomic mass of the sample [Hu *et al.*, 2003]. The procedure of deriving  $V_P$ ,  $V_S$ , and  $G$  from the  $V_D$  and equation of state

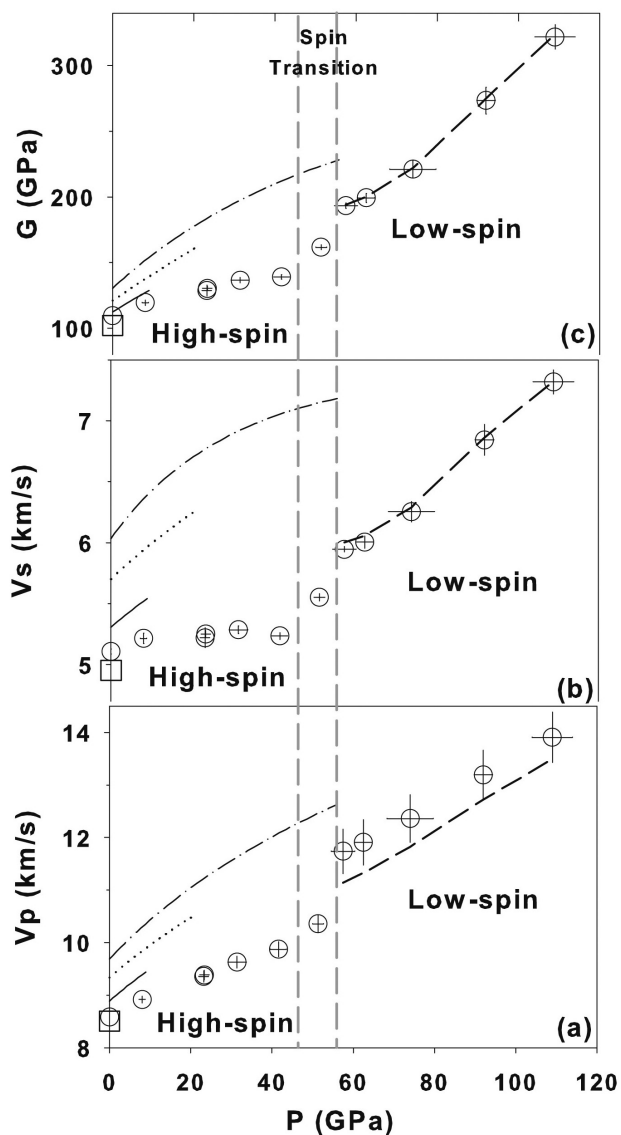


**Figure 2.** Aggregate (a)  $V_P$ , (b)  $V_S$ , and (c)  $G$  of  $(\text{Mg}_{0.75}, \text{Fe}_{0.25})\text{O}$  at high pressures. Open circles: this study based on the Birch-Murnaghan EOS [Birch, 1986] of Lin *et al.* [2005]; Dashed lines: this study based on the  $K_S$  and its pressure derivative of MgO with the density of  $(\text{Mg}_{0.75}, \text{Fe}_{0.25})\text{O}$  [Fei *et al.*, 2005]; Dash-dotted lines:  $V_P$ ,  $V_S$ , and  $G$  of MgO [Zha *et al.*, 2000]; Dotted lines:  $(\text{Mg}_{0.94}, \text{Fe}_{0.06})\text{O}$  from Brillouin measurements [Jackson *et al.*, 2006]; Solid lines:  $(\text{Mg}_{0.83}, \text{Fe}_{0.17})\text{O}$  from previous ultrasonic measurements [Kung *et al.*, 2002]; Open squares:  $V_P$ ,  $V_S$ , and  $G$  of single-crystal  $(\text{Mg}_{0.76}, \text{Fe}_{0.24})\text{O}$  at ambient conditions from previous ultrasonic measurements [Jacobsen *et al.*, 2002]; Vertical gray lines: observed transition region. The difference in the  $V_P$  between the high-spin and low-spin ferropericlasite at approximately 60 GPa is from 1.53 km/s (open circles) to 0.78 km/s (dash lines) (Figure 2a). The pressure derivative of the shear modulus for the low-spin  $(\text{Mg}_{0.75}, \text{Fe}_{0.25})\text{O}$  above 60 GPa is approximately 2.55, which is higher than that of the high-spin ferropericlasite [Kung *et al.*, 2002; Jackson *et al.*, 2006]. As shown, the derived  $V_S$  and  $G$  values are very insensitive to the input EOS parameters. Errors in this study are based on the statistics of the data, and some error bars are smaller than the symbol size.

(EOS) parameters, namely the adiabatic bulk modulus ( $K_S$ ) and density ( $\rho$ ), has been described previously [Hu *et al.*, 2003; Mao *et al.*, 2004]. Here we used the EOS parameters for the high-spin and low-spin ferroperricite from a recent

X-ray diffraction study [Lin *et al.*, 2005] using Birch-Murnaghan EOS [Birch, 1986]; the  $K_S$  and its pressure derivative of MgO with the density of  $(\text{Mg}_{0.75}, \text{Fe}_{0.25})\text{O}$  was also used to calculate the  $V_P$ ,  $V_S$ , and  $G$  for the low-spin ferroperricite and to understand the potential influence of the input EOS on the derived parameters, because a separate X-ray diffraction study indicates that the compression curves of the low-spin phases in various  $(\text{Mg}, \text{Fe})\text{O}$  compositions are similar to that of MgO [Fei *et al.*, 2005]. We note that the NRIXS technique is particularly well suited for constraining  $V_S$  and  $G$  from a precise measurement of  $V_D$  because they are considerably less sensitive to the choice of EOS input data ( $K_S$ ,  $\rho$ ) compared with  $V_P$  [Mao *et al.*, 2004] (Figure 2); though, uncertainties in the input EOS parameters due to non-hydrostatic stress in the sample and kinetic hysteresis of the spin transition at ambient temperature can propagate into the model in deriving the  $V_P$ ,  $V_S$ , and  $G$ .

[7] Under ambient conditions, our  $V_P$ ,  $V_S$ , and  $G$  values are consistent with previous ultrasonic measurements (Figure 2) [Jacobsen *et al.*, 2002], verifying the procedure for deriving sound velocities from PDOS. Compared with MgO [Zha *et al.*, 2000], addition of 25 atom% FeO into MgO significantly reduces the value of  $V_P$ ,  $V_S$ , and  $G$  for the high-spin ferroperricite, while the value of  $K_S$  is unchanged within experimental uncertainties [Jacobsen *et al.*, 2002, 2004; Kung *et al.*, 2002; Jackson *et al.*, 2006; Lin *et al.*, 2005]. An abnormal behavior in the sound velocities and shear modulus in  $(\text{Mg}_{0.75}, \text{Fe}_{0.25})\text{O}$  occurs between 42 GPa and 58 GPa (Figure 2). The high-pressure low-spin ferroperricite exhibits a much higher  $V_P$ ,  $V_S$ , and  $G$  than the low-pressure high-spin ferroperricite (Figure 2), consistent with a discontinuous pressure-volume profile measured by a recent high-pressure X-ray diffraction study [Lin *et al.*, 2005]. An additional important observation is that there is a significant increase in the pressure derivatives of the  $V_P$ ,  $V_S$ , and  $G$  for the low-spin ferroperricite, as compared to the high-spin ferroperricite; i.e., assuming a linear pressure dependence, the pressure derivatives of the  $V_P$ ,  $V_S$ , and  $G$  for the low-spin  $(\text{Mg}_{0.75}, \text{Fe}_{0.25})\text{O}$  above 60 GPa are approximately 0.0427 (km/sGPa), 0.0274 (km/sGPa), and 2.55, respectively. Based on these observations, simple extrapolations of the  $V_P$ ,  $V_S$ , and  $G$  for the high-spin ferroperricite would yield much lower values than that of

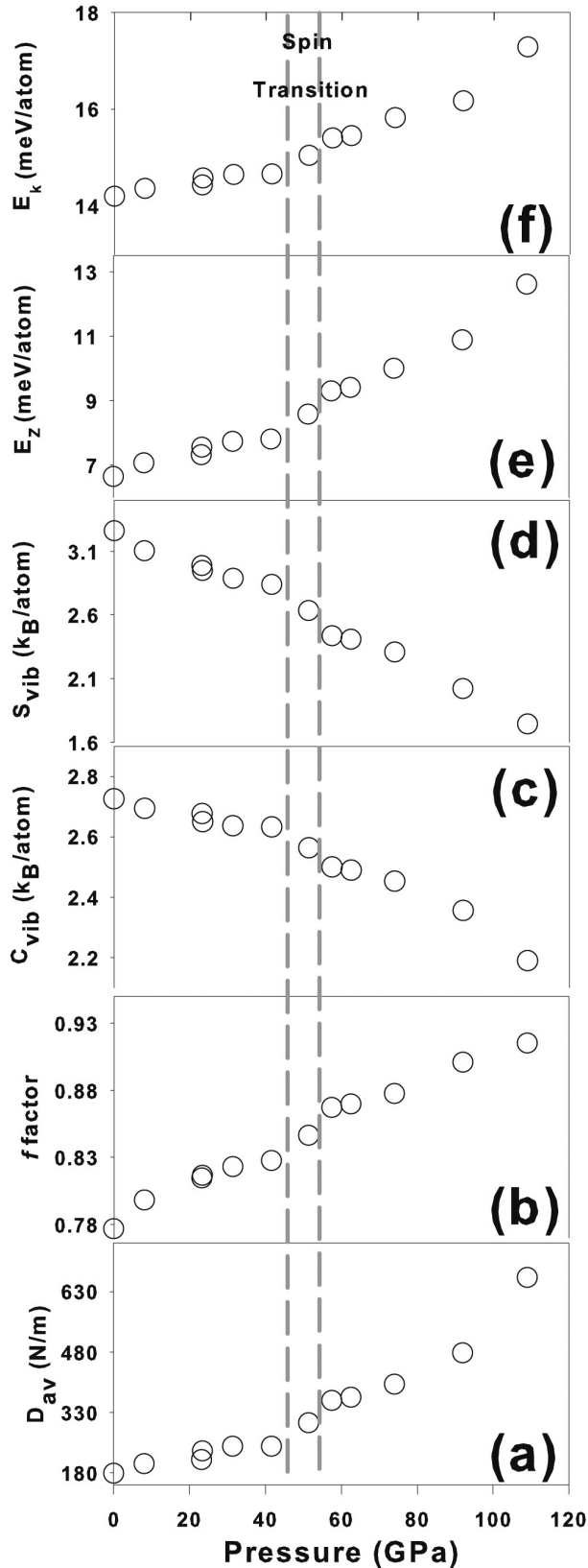


**Figure 3.** Elastic, thermodynamic, and vibrational parameters of  $(\text{Mg}_{0.75}, \text{Fe}_{0.25})\text{O}$  as a function of pressure obtained from integration of the PDOS. (a) Mean force constant,  $D_{av}$ ; (b) Lamb-Mössbauer factor,  $f_{LM}$ ; (c) vibrational specific heat,  $C_{vib}$  ( $k_B$ , Boltzmann constant); (d) vibrational entropy,  $S_{vib}$ ; (e) kinetic energy at 0 K,  $E_Z$ ; (f) kinetic energy,  $E_k$ . We note that these values only represent the contribution of the Fe sublattice in  $(\text{Mg}_{0.75}, \text{Fe}_{0.25})\text{O}$ . The observed increase in the mean force constant across the spin-pairing transition indicates an increase in the interatomic force constant and hence the observed jump in the bulk modulus, consistent with the increase in the bulk modulus reported by a recent X-ray diffraction study [Lin *et al.*, 2005]. An increase in the  $f_{LM}$  also indicates a much reduced displacement of iron atoms and stiffening in the low-spin  $(\text{Mg}_{0.75}, \text{Fe}_{0.25})\text{O}$ .



the low-spin ferropericlasite at lowermost mantle pressures (Figure 2).

[8] The electronic spin-pairing transition of iron is also found to significantly influence other elastic, thermodynamic and vibrational properties of the iron component in ( $\text{Mg}_{0.75}, \text{Fe}_{0.25}$ )O (Figure 3); the mean force constant ( $D_{av}$ ), Lamb-Mössbauer factor ( $f_{LM}$ ), kinetic energy ( $E_k$ ), and kinetic energy at 0 K ( $E_z$ ) all increase while vibrational specific heat ( $C_{vib}$ ) and vibrational entropy ( $S_{vib}$ ) decrease across the electronic transition at  $\sim 50$  GPa.

#### 4. Geophysical Applications

[9] The dramatic jump of the sound velocities of ferropericlasite across the electronic spin-pairing transition reported here has important implications for the geophysics of the Earth's lower mantle. Earlier measurements of the sound velocities of ferropericlasite and silicate perovskite under high pressures and/or high temperatures have been used to constrain the geophysics and geochemistry of the lower mantle; however, these studies for ferropericlasite were limited to the high-spin state at pressures below 20 GPa (lower than the pressures of the lower mantle) [Jacobsen *et al.*, 2002, 2004; Kung *et al.*, 2002; Jackson *et al.*, 2006]. These studies have shown that the  $V_P$  and  $V_S$  of these minerals are too high to match the seismic model of the lower mantle, specifically above 60 to 70 GPa (approximately 1500 km in depth); thus far, these systematic deviations cannot be accounted for by temperature effects alone [Trampert *et al.*, 2004; Wentzcovitch *et al.*, 2004; Mattern *et al.*, 2005; Jackson *et al.*, 2006]. Although the nature of the electronic spin-pairing transition under high temperatures of the Earth's lower mantle has yet to be understood experimentally, recent theoretical predictions suggest that the transition in ferropericlasite would occur over an extended pressure range of approximately 30 GPa (or  $\sim 700$  km in depth) [Sturhahn *et al.*, 2005; Tsuchiya *et al.*, 2006]. In this case, the associated increase in the  $V_P$ ,  $V_S$ ,  $G$ ,  $K_S$ , and their pressure derivatives across a gradual spin crossover in ferropericlasite would gradually increase the mismatch between the synthetic pyrolite model and PREM. That is, the sound velocities of the low-spin ferropericlasite need to be considered in future geophysical and geochemical models in determining mineralogy and chemistry of the lower mantle [e.g., Kellogg *et al.*, 1999; van der Hilst and Kárason, 1999; Trampert *et al.*, 2004; Wentzcovitch *et al.*, 2004; Mattern *et al.*, 2005]. In particular, the effect of the electronic spin-pairing transition on the sound velocities could offset the effect of the addition of iron in the lower mantle minerals (Figure 2), affecting the evaluation of the lower mantle chemical heterogeneities [Trampert *et al.*, 2004].

[10] Electronic spin-pairing transitions of iron have also been observed to occur in silicate perovskite [Badro *et al.*, 2004; Li *et al.*, 2004; Jackson *et al.*, 2005; Hofmeister, 2006], though the transitions are more complex than in ferropericlasite. Based on the two-step, gradual electronic transitions and the lesser amount of iron in silicate perovskite (approximately 10%) [Murakami *et al.*, 2005], it remains to be seen how the electronic transitions of iron, if present in the lower mantle [Hofmeister, 2006], affect the sound velocities of silicate perovskite in the lower mantle. It

also remains to be seen how high temperature affects the elastic, thermodynamic, and transport properties of the low-spin ferropericlasite under lower mantle conditions [Sturhahn *et al.*, 2005; Tsuchiya *et al.*, 2006; Goncharov *et al.*, 2006], but the sound velocities we report here for ferropericlasite across the spin-pairing transition indicate that previous models of lower-mantle sound velocities from mineral physics data using high-spin ferropericlasite and silicate perovskite are insufficient to correctly model the seismic wave behavior in the lower mantle.

[11] **Acknowledgments.** We acknowledge XOR-3, APS, ANL for the use of the synchrotron facilities and HPCAT for the use of the ruby system. We thank V. V. Struzhkin, Y. Fei, V. Iota, and H. C. Cynn for their fruitful discussions. We wish to thank E. E. Alp for designing the new Be gaskets. This work and use of the APS are supported by U.S. DOE, Basic Energy Sciences, Office of Science, under contract W-31-109-ENG-38, and the State of Illinois under HECA. This work at LLNL was performed under the auspices of the U.S. DOE by University of California and LLNL under contract W-7405-Eng-48. J.F.L. is also supported by the Lawrence Livermore Fellowship. S.D.J. acknowledges financial support from NSF EAR-0440112, a Carnegie Fellowship and CDAC.

#### References

- Badro, J., *et al.* (2003), Iron partitioning in Earth's mantle: Toward a deep lower mantle discontinuity, *Science*, *300*, 789–791.
- Badro, J., *et al.* (2004), Electronic transitions in perovskite: Possible non-conducting layers in the lower mantle, *Science*, *305*, 383–386.
- Birch, F. (1986), Equation of state and thermodynamic parameters of NaCl to 300 kbar in the high-temperature domain, *J. Geophys. Res.*, *91*, 4949–4954.
- Dziewonski, A. M., and D. L. Anderson (1981), Preliminary reference Earth model, *Phys. Earth Planet. Inter.*, *25*, 297–356.
- Fei, Y., *et al.* (2005), Spin transition in (Mg,Fe)O at high pressure, *Eos Trans. AGU*, *86*(52), Fall Meet. Suppl., Abstract MR14A-05.
- Goncharov, A. F., V. V. Struzhkin, and S. D. Jacobsen (2006), Reduced radiative conductivity of low-spin (Mg, Fe)O in the lower mantle, *Science*, *312*, 1205–1208.
- Hofmeister, A. M. (2006), Is low-spin  $\text{Fe}^{2+}$  present in Earth's mantle?, *Earth Planet. Sci. Lett.*, *243*, 44–52.
- Hu, M., *et al.* (2003), Measuring velocity of sound with nuclear resonant inelastic x-ray scattering, *Phys. Rev. B*, *67*, 094304.
- Jackson, I. (1998), Elasticity, composition and temperature of the Earth's lower mantle: A reappraisal, *Geophys. J. Int.*, *134*, 291–311.
- Jackson, J. M., *et al.* (2005), A synchrotron Mössbauer spectroscopy study of (Mg,Fe)SiO<sub>3</sub> perovskite up to 120 GPa, *Am. Mineral.*, *90*, 199–205.
- Jackson, J. M., S. V. Sinogeikin, S. D. Jacobsen, H. J. Reichmann, S. J. Mackwell, and J. D. Bass (2006), Single-crystal elasticity and sound velocities of (Mg<sub>0.94</sub>Fe<sub>0.06</sub>)O ferropericlasite to 20 GPa, *J. Geophys. Res.*, *111*, B09203, doi:10.1029/2005JB004052.
- Jacobsen, S. D., H. J. Reichmann, H. A. Spetzler, S. J. Mackwell, J. R. Smyth, R. J. Angel, and C. A. McCammon (2002), Structure and elasticity of single-crystal (Mg, Fe)O and a new method of generating shear waves for gigahertz ultrasonic interferometry, *J. Geophys. Res.*, *107*(B2), 2037, doi:10.1029/2001JB000490.
- Jacobsen, S. D., H. Spetzler, H. J. Reichmann, and J. R. Smyth (2004), Shear waves in the diamond-anvil cell reveal pressure-induced instability in (Mg, Fe)O, *Proc. Natl. Acad. Sci. U.S.A.*, *100*, 5867–5871.
- Kellogg, L. H., B. H. Hager, and R. D. van der Hilst (1999), Compositional stratification in the deep mantle, *Science*, *283*, 1881–1884.
- Kung, J., B. Li, D. J. Weidner, J. Zhang, and R. C. Liebermann (2002), Elasticity of (Mg<sub>0.83</sub>, Fe<sub>0.17</sub>)O ferropericlasite at high pressure: Ultrasonic measurements in conjunction with X-radiation techniques, *Earth Planet. Sci. Lett.*, *203*, 557–566.
- Li, B., and J. Zhang (2005), Pressure and temperature dependence of elastic wave velocity of MgSiO<sub>3</sub> perovskite and the composition of the lower mantle, *Phys. Earth Planet. Inter.*, *151*, 143–154.
- Li, J., *et al.* (2004), Electronic spin state of iron in lower mantle perovskite, *Proc. Natl. Acad. Sci. U.S.A.*, *101*, 14,027–14,030.
- Lin, J. F., J. Shu, H. K. Mao, R. J. Hemley, and G. Shen (2003), Amorphous boron gasket in diamond anvil cell research, *Rev. Sci. Instrum.*, *74*, 4732–4736.
- Lin, J. F., *et al.* (2005), Spin transition of iron in magnesiowüstite in Earth's lower mantle, *Nature*, *436*, 377–380.
- Lin, J. F., *et al.* (2006), Pressure-induced electronic spin transition of iron in magnesiowüstite- (Mg, Fe)O, *Phys. Rev. B*, *73*, 113107.

- Mao, W. L., W. Sturhahn, D. L. Heinz, H.-K. Mao, J. Shu, and R. J. Hemley (2004), Nuclear resonant x-ray scattering of iron hydride at high pressure, *Geophys. Res. Lett.*, *31*, L15618, doi:10.1029/2004GL020541.
- Mattern, E., J. Matas, Y. Ricard, and J. Bass (2005), Lower mantle composition and temperature from mineral physics and thermodynamic modeling, *Geophys. J. Int.*, *160*, 973–990.
- Murakami, M., K. Hirose, N. Sata, and Y. Ohishi (2005), Post-perovskite phase transition and mineral chemistry in the pyrolytic lowermost mantle, *Geophys. Res. Lett.*, *32*, L03304, doi:10.1029/2004GL021956.
- Speziale, S., et al. (2005), Iron spin transition in Earth's mantle, *Proc. Natl. Acad. Sci. U.S.A.*, *102*, 17,918–17,922.
- Sturhahn, W. (2004), Nuclear resonant spectroscopy, *J. Phys. Condens. Matter*, *16*, S497.
- Sturhahn, W., J. M. Jackson, and J. F. Lin (2005), The spin state of iron in minerals of Earth's lower mantle, *Geophys. Res. Lett.*, *32*, L12307, doi:10.1029/2005GL022802.
- Trampert, J., F. Deschamps, J. Resovsky, and D. Yuen (2004), Probabilistic tomography maps chemical heterogeneities throughout the lower mantle, *Science*, *306*, 853–856.
- Tsuchiya, T., R. M. Wentzovitch, C. R. S. da Silva, and S. de Gironcoli (2006), Spin transition in magnesiowüstite in Earth's lower mantle, *Phys. Rev. Lett.*, *96*, 198501.
- van der Hilst, R. D., and H. Kárason (1999), Compositional heterogeneity in the bottom 1000 kilometers of Earth's mantle: Toward a hybrid convection model, *Science*, *283*, 1885–1888.
- Wentzovitch, R. M., B. B. Karki, M. Cococcioni, and S. de Gironcoli (2004), Thermoelastic properties of MgSiO<sub>3</sub>-perovskite: insights on the nature of the Earth's lower mantle, *Phys. Rev. Lett.*, *92*, 018501.
- Zha, C. S., H. K. Mao, and R. J. Hemley (2000), Elasticity of MgO and a primary pressure scale to 55 GPa, *Proc. Natl. Acad. Sci. U.S.A.*, *97*, 13,494–13,499.

---

J. M. Jackson, Division of Geological and Planetary Sciences, California Institute of Technology, 1200 California Blvd., Pasadena, CA 91125, USA.

S. D. Jacobsen, Department Earth and Planetary Sciences, Northwestern University, 1850 Campus Drive, Evanston, IL 60208, USA.

J.-F. Lin and C.-S. Yoo, Lawrence Livermore National Laboratory, 7000 East Avenue, Livermore, CA 94550, USA. (afu@llnl.gov)

W. Sturhahn and J. Zhao, Advanced Photon Source, Argonne National Laboratory, 9700 South Cass Avenue, Argonne, IL 60439, USA.